Plant Reproduction
https://doi.org/10.1007/s00497-021-00406-3

ORIGINAL ARTICLE

Transgenerational conditioned male fertility of HD-ZIP IV transcription factor mutant *ocl4*: impact on 21-nt phasiRNA accumulation in pre-meiotic maize anthers

Pranjal Yadava[1,2,6] · Saleh Tamim[3] · Han Zhang[1] · Chong Teng[4] · Xue Zhou[1] · Blake C. Meyers[4,5] · Virginia Walbot[1]

Received: 19 July 2020 / Accepted: 8 February 2021

Abstract

Key message **Maize** ***Outer cell layer 4 (ocl4)*** **encodes an HD-ZIP IV transcription factor required for robust male fertility and 21-nt phasiRNA biogenesis.** ***ocl4*** **fertility is favored in warm conditions, and phasiRNAs are partially restored.**

Abstract Environment-sensitive male-sterile plants have been described before and can result from different molecular mechanisms and biological processes, but putative environment-conditioned, transgenerational rescue of their male fertility is a rather new mystery. Here, we report a derivative line of the male-sterile *outer cell layer 4* (*ocl4*) mutant of maize, in which fertility was restored and perpetuated over several generations. Conditioned fertile *ocl4* anthers exhibit the anatomical abnormality of a partially duplicated endothecial layer, just like their sterile counterparts. We profiled the dynamics of phased, small interfering RNAs (phasiRNAs) during pre-meiotic development in fully sterile and various grades of semi-fertile *ocl4* anthers. The conditioned fertile anthers accumulated significantly higher 21-nt phasiRNAs compared to *ocl4* sterile samples, suggesting a partial restoration of phasiRNAs in conditioned fertility. We found that the biogenesis of 21-nt phasiRNAs is largely dependent on *Ocl4* at three key steps: (1) production of *PHAS* precursor transcripts, (2) expression of miR2118 that modulates precursor processing, and (3) accumulation of 21-nt phasiRNAs.

Keywords Male sterility · Conditioned fertility · PhasiRNA · *Ocl4* · Maize

Communicated by David Twell.

Pranjal Yadava and Saleh Tamim have contributed equally to this work.

✉ Virginia Walbot
walbot@stanford.edu

1 Department of Biology, Stanford University, Stanford, CA 94305, USA

2 Indian Council of Agricultural Research-, Indian Institute of Maize Research, Pusa Campus, New Delhi 110012, India

3 Center for Bioinformatics and Computational Biology, University of Delaware, Newark, DE 19711, USA

4 Donald Danforth Plant Science Center, 975 N. Warson Rd, St. Louis, MO 63132, USA

5 Division of Plant Sciences, University of Missouri, 52 Agriculture Building, Columbia, MO 65201, USA

6 Present Address: Division of Plant Physiology, Indian Agricultural Research Institute, Pusa, New Delhi 110012, India

Introduction

The maize genome encodes 17 homeodomain leucine zipper type IV (HD-ZIP IV) proteins whose transcripts preferentially accumulate in the epidermis (Sosso et al. 2010; Javelle et al. 2011). Nine family members are expressed in immature tassels: four types are encoded by duplicated genes, while *outer cell layer 4* (*Ocl4*) is a single-copy gene (Javelle et al. 2011). *Ocl4* is expressed in diverse epidermal cell types in multiple organs in addition to the tassel (Javelle et al. 2011). The *ocl4-1* mutant allele is disrupted by a *Mu8* insertion in exon 6, and the plants are male sterile attributed to a duplicated endothecial layer; mutant plants accumulate fewer transcripts than normal, some transcripts are alternatively spliced, and *ocl4-1* is predicted to encode a truncated partial or complete loss-of-function protein (Vernoud et al. 2009).

During fertile male development, pre-meiotic archesporial cells are specified centrally in each of the four anther lobes. These cells secrete MAC1 protein, a signal that

Published online: 10 March 2021

triggers somatic differentiation of neighboring cells forming a ring of primary parietal cells (PPC); these somatic cells then divide periclinally to produce the subepidermal endothecium and the secondary parietal cells adjacent to the archesporial cells (Wang et al. 2012; Dukowic-Schulze and van der Linde 2021). This division also marks an exit from pluripotency in the soma (Kelliher and Walbot 2014). In *ocl4* mutants, the earliest steps of anther development are normal; however, lobe architecture deviates after the PPC periclinal division. In the outer hemisphere of each lobe, underlying the epidermal domain of *Ocl4* expression, endothecial cells undergo an ectopic periclinal division producing a bilayer (Vernoud et al. 2009). The bilayer defect is cytologically complete about the third day of maize anther development (0.4 mm anther length), and it has been proposed that epidermal cells produce a signal to repress endothecial periclinal cell division (Wang et al. 2012). Generally, *ocl4-1* plants are male sterile but were reported to show sporadic partial fertility under greenhouse growing conditions (24 °C /19 °C and 16-h light/8-h dark), while male sterility was observed in more variable field conditions (Vernoud et al. 2009). A second striking phenotype of *ocl4-1* mutants is the emergence of ectopic macro hairs in novel zones of the leaf, supporting a hypothesis that OCL4 is required to repress this epidermal structure in specific leaf domains.

Maize anthers of 0.4 mm size are notable for the high accumulation of 21-nt, phased, small interfering RNAs (phasiRNAs) that peak in abundance at this pre-meiotic stage (Zhai et al. 2015). First described in the grasses (Johnson et al. 2009), male reproductive tissues of diverse angiosperms accumulate two size classes of 21- and 24-nucleotide (nt) phasiRNAs (Zheng et al. 2015; Xia et al. 2019). The similarity of phasiRNAs and mammalian piRNAs (*P*-element induced wimpy testis—interacting RNAs) may be a case of convergent evolution in support of male reproduction (Zhai et al. 2015). The shared characteristics include a high abundance in male reproductive organs, two distinct size classes, phased production from noncoding precursors, and generation in somatic cells. Even as the precise direct functions of these RNA species were largely unknown until recently, the absence or perturbation of mammalian piRNAs or grass phasiRNAs is often associated with male sterility. Recent evidences show that rice 21-nt phasiRNAs are capable of reprogramming gene expression during meiotic progression, could act in a target-cleavage mode, and may be responsible for facilitating the progression of meiosis by fine-tuning carbohydrate biosynthesis and metabolism in male germ cells (Zhang et al. 2020; Jiang et al. 2020).

Plant phasiRNAs originate from 5′-capped and polyadenylated, noncoding mRNA precursors (*PHAS* transcripts) that are generated by RNA polymerase II (Pol II). The precursors are derived from non-repetitive genomic loci. Precursor processing is initiated by the binding of a microRNA (miRNA) "trigger": miR2118 for 21-nt *PHAS* loci transcripts and miR2275 for 24-nt *PHAS* loci. miRNA binding is required for Argonaute-mediated cleavage of the precursor, and the resulting 3′ fragment is converted to a double-stranded substrate by RNA-DEPENDENT RNA POLYMERASE 6 (RDR 6). The dsRNA is then cleaved at precise intervals by a Dicer-like enzyme: DCL4 generates 21-nt phasiRNAs, and DCL5 produces the 24-nt class. OCL4 is a key regulator of 21-nt phasiRNA biogenesis: It is required for robust production of *PHAS* precursor transcripts, normal levels of miR2118, and accumulation of 21-nt phasiRNAs (Zhai et al. 2015).

Nuclear-controlled, environment-sensitive, genic male sterility (EGMS) is a trait exploited by plant breeders, most successfully in rice. The molecular bases of this trait in rice in some lines have only recently been determined (Kim and Zhang 2018). The underlying mechanisms and players controlling this trait mainly include epigenetic regulation, transcription factors, and noncoding RNAs. The rice PA64 male-sterile line exhibits higher DNA methylation levels under long-day and high-temperature conditions (Chen et al. 2014), whereas small RNAs, long noncoding RNAs, and/or RNA-directed DNA methylation play a role in regulating photoperiod-sensitive male sterility in Nongken 58S rice (Ding et al. 2012a, b; Kim and Zhang 2018; Fan et al. 2016). The temperature-sensitive male sterility in the HengnongS-1 rice genotype results from a recessive single nucleotide polymorphism (SNP) within *PERSISTANT TAPETAL CELL 1*(*PTC1*), which encodes a PHD-finger protein involved in tapetal cell death and pollen development (Li et al. 2011; Qi et al. 2014). A mutation in the R2R3 MYB transcription factor, CARBON STARVED ANTHER, shows complete male sterility under short-day conditions, but is fertile under long-day conditions (Zhang et al. 2010, 2013). Further, UDP-glucose pyrophosphorylase 1 (*Ugp-1*) co-suppression rice lines are male sterile under normal temperatures because endogenous *Ugp1* transcripts are not spliced, but revert to being male fertile at low temperatures because of more efficient splicing of the primary *Ugp1* mRNA (Chen et al. 2007). One additional example is from the wheat line BS366, which is male sterile at 10 °C and fertile at 20 °C; this line shows differential expression of miRNAs involved in modulating auxin and gibberellin signaling pathways for the male fertility transition (Bai et al. 2017). It is clear that there are multiple pathways in which mutations can yield environment-conditioned male fertility.

Of particular relevance to our work are EGMS traits involving 21-nt phasiRNAs and/or long noncoding RNAs (lncRNAs). Photoperiod-sensitive male sterility in Nongken 58S rice is controlled in part by a 21-nt phasiRNA-producing locus (*Pms1*) that generates the *PMS1T* precursor transcript. *PMS1T* has a miR2118 target site and is processed to form abundant 21-nt phasiRNAs. Nongken 58S has a SNP

in *PMS1T* near the miR2118 recognition site, and under long-day photoperiod conditions, this genotype is male sterile (Fan et al. 2016). A second locus, *Pms3*, encodes a lncRNA that is also processed into small RNAs (Ding et al. 2012a; Zhou et al. 2012). A SNP in *pms3* promotes increased siRNA-directed methylation within its promoter region, leading to reduced transcript levels and consequent sterility, specifically under long-day conditions (Ding et al. 2012a; Zhou et al. 2012).

To date, no individual 21-nt *PHAS* locus has been associated with male sterility in maize. The *ocl4* mutants lack nearly all 21-nt phasiRNAs (Zhai et al. 2015). *dcl5* mutants lack most 24-nt phasiRNAs and are male sterile under optimal, warm growing conditions (28 °C/ 22 °C, 16-h days/8-h nights in the greenhouse). Under cool growing conditions, fertility is restored in the absence of 24-nt phasiRNAs. Consequently, *dcl5* represents a case of EGMS. *Dcl5* is preferentially present in the tapetum; *dcl5* mutants show delayed tapetal development, starting in early meiosis (Teng et al. 2020). Combining our current knowledge about rice *pms1, pms3,* and maize *dcl5*, we suggest that reproductive phasiRNAs buffer development under variable or unfavorable environmental conditions.

Here, we describe an *ocl4//ocl4* derivative line, in which fertility was restored and perpetuated over several generations, under warm growing conditions. We designate this line as "conditioned fertile *ocl4*" as its fertility was putatively conditioned by a heat wave. We present a genetic, phenotypic, RNA-seq, and small RNA-seq assessment of male-sterile *ocl4* and conditioned fertile *ocl4* anthers, in an effort to better understand the role of 21-nt phasiRNAs in male reproduction. Our results indicate that conditioned male fertility of *ocl4* is associated with enhanced 21-nt phasiRNA accumulation in pre-meiotic maize anthers, while the anthers retained all canonical features of sterile *ocl4* cellular organization.

Results

Ocl4 maintains male fertility under cooler conditions

The *ocl4-1* allele in the A188 background (87.5% A188) was a gift of V. Vernoud prior to publication (Vernoud et al. 2009) for use in allelism testing of a panel of 55 new cases of recessive male sterility (Timofejeva et al. 2013). A line segregating 1:1 fertile/sterile was established and maintained by male-sterile (*ocl4//ocl4*) × heterozygous fertile (*ocl4//+*) crosses within a family for three field generations. Both the sterile and fertile individuals were used in complementation crosses to test for allelism in the new panel of male-sterile mutants. After the test cross, F_1 progeny were observed for sterility in the subsequent summer field. In complemented families (no male sterility), several self-pollinations were performed to derive double mutant stocks. No unusual segregation ratios were observed in crosses involving *ocl4-1* over the course of several years (Timofejeva et al. 2013).

During the multi-year propagation of *ocl4-1,* we identified homozygous *ocl4* mutant plants that were male fertile. In the subsequent generation after self-pollination of a fertile homozygote, the progeny family was nearly all fertile. For subsequent analysis, we focused on an individual (ZM68-10), which was *ocl4//ocl4* double mutant by genotype, but still fertile in phenotype (see Materials and Methods, Fig. 1). Progeny of ZM68-10 (×) were 36F:0 ms in the 2015 field season, and the ZM68-2 ms × ZM68-10 progeny were

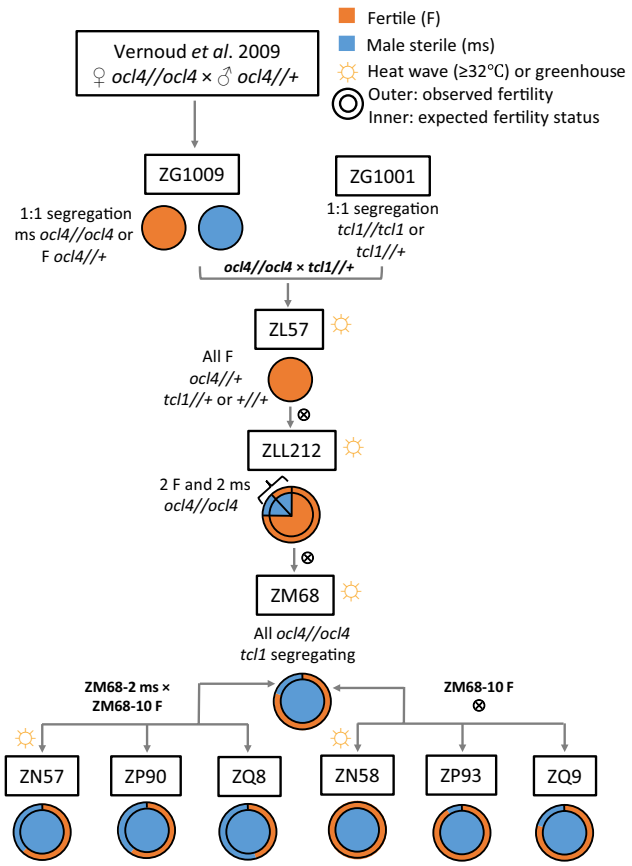

Fig. 1 Derivation, propagation, and phenotypic analysis of *ocl4* homozygous plants. Among the families, only ZLL212 plants were grown in the greenhouse; all others were planted in the summer field. Heat waves occurred in late June during the ZL to ZN generations, coincident with the time of action of OCL4 regulation of 21-nt phasiRNAs and endothecium development. All ZM68 individuals were test crossed to *tcl1//tcl1* male-sterile homozygotes to identify individuals that were not carriers (+//+, not tcl//+); only progeny of ZM68 non-carriers were utilized in subsequent analysis of *ocl4//ocl4* homozygotes. Orange color: fertile (F) plants; blue color: male sterile (ms) plants. Starting with the ZLL generation, the inner circle depicts the expected phenotype (F or ms), and the outer circle is the observed fertility status

28F:17 ms. These results indicate that the switch to fertility can persist, but it is not a complete switch to full fertility. We wondered whether it reflected a genetic change in the ZM68-10 lineage. We considered the possibility that we had selected a new *ocl4* allele. Evaluation of RNA-seq data of derivative progeny indicated that the original *ocl4-1* allele was still present (Online Resource 1 Fig. S1), as described in detail in the subsequent section.

We next considered environmental parameters. *ocl4-1* lines were planted in May each year, and the most advanced anthers in a tassel would reach the 1.25 mm stage (prophase I of meiosis) by the end of June, about 38 days after planting. Each tassel contains anthers spanning about 5 days of development in the A188 background; consequently, the youngest anthers would be at the 0.4 mm stage in the same tassel. Stanford typically has cool late June growing conditions of 22–24 °C daytime and 12–15 °C night temperatures, punctuated by one day of much cooler or much hotter weather. Both the 2014 and 2015 growing seasons experienced heat waves at the end of June, while subsequent years had the typical cool growing conditions present during the complementation crosses earlier (Online Resource 2 Table S1). Under heat wave conditions, the ZM68-10 (×) progeny were all fertile (36F:0 ms), but under cooler conditions, the families were 64F:9 ms. For ZM68-2 ms × ZM68-10, under heat wave conditions, the ratio was 28F:17 ms, but under cool conditions, 28F:24 ms. These results are indicative of EGMS—that is, higher temperatures favor fertility. Additionally, there appeared to be an epigenetic component, in that the putative epialleles in the ZM68-10 plant were highly responsive to heat, whereas the allele from the ZM68-2 plant was non-responsive or less responsive. This is an unexpected complication to EGMS and could involve a change in a locus other than *ocl4*.

Conditioned fertile *ocl4* anthers retain a partially duplicated endothecial layer and exhibit a range of fertility levels

The observed restoration of fertility motivated a more detailed investigation of the extent of fertility in *ocl4-1* sterile compared to *ocl4-1* conditioned fertile plants. To achieve this, we used a scoring system to assess plant fertility by comparing the number of anthers in *ocl4* plants relative to normal *Ocl4* plants in families segregating 1:1 fertile: male sterile. Full fertility was assigned a score of 5, and complete sterility a score of 0. Conditioned fertile *ocl4//ocl4* plants exhibited a range of fertility levels from 1 to 4 in the 2018 field season (Fig. 2a). We ascribe the phenotypic range to responses of cohorts of developing anthers to temperature conditions at a phenocritical stage (Online Resource 2 Table S1). We used the material with graded fertility scores for genotyping, anther dissection, and RNA preparation as indicated in Table 1.

The defining anatomical defect of the *ocl4* mutant is a partially duplicated endothecial layer in anther lobes. Using confocal microscopy, we found that the conditioned fertile *ocl4* retains this defect (Fig. 2b). In pre-meiotic *Ocl4* anthers, the expected architecture of a three-layer cell wall (epidermis, endothecium, secondary parietal layer) is present at 0.5 mm, but by 0.7 mm and completing by 1.0 mm, the normal four-layer cell wall exists after periclinal division of the secondary parietal cells to form the middle layer and tapetum. In contrast, in both *ocl4* sterile and *ocl4* conditioned fertile mutants, two cell layers with endothecial cell shape characteristics were gradually generated after extra periclinal cell divisions in the presumptive endothecial layer, resulting in five somatic cell layers by 1.0 mm (Fig. 2b) in the distal hemisphere of each lobe as previously described (Vernoud et al.2009; Wang et al. 2012).

Previously, this extra subepidermal cell layer has been cited as the cause of pollen failure in *ocl4* mutants. Our findings question this link between a partial extra endothecial layer and male sterility. We cannot be definitive, however, because at the time of anther analysis, it is unknown whether a particular anther will be fertile or sterile. As shown in Fig. 2a, there is a range of partial fertility in *ocl4* homozygous plants; it is possible that the confocal microscopy was of anthers destined to be sterile.

Conditioned fertile *ocl4* anthers show higher accumulation of 21-nt phasiRNAs

Our observation of conditioned fertile *ocl4* anthers motivated us to assess the impact of *ocl4* on small RNAs in general and phasiRNAs in particular, given their known connection to male sterility. We built libraries and sequenced samples from *ocl4* conditioned fertile anthers at pre-meiotic stages (anthers length ranging from 0.4 to 0.7 mm) grown under normal controlled conditions in greenhouse to compare with previously published *ocl4* sterile and wild-type samples, that were also grown in same normal controlled conditions in greenhouse (Online Resource 2 Table S2). We first looked at the populations of different small RNA classes categorized by length to determine classes that are predominant and that are significantly impacted in the two *ocl4* conditions. We found the 21- and 24-nt small RNA classes to be the predominant classes across all samples (Fig. 3a). We observed a slight increase in the 24-nt sRNAs in the *ocl4* samples, but as expected, the proportions of small RNA classes across genotypes were overwhelmingly from repeat regions of the genome (Fig. 3a; Online Resource 1 Fig. S2). Unlike the 24-nt class, we saw a significant reduction in small RNA abundance for the 21-nt class in both *ocl4* sterile and conditioned fertile samples compared to the

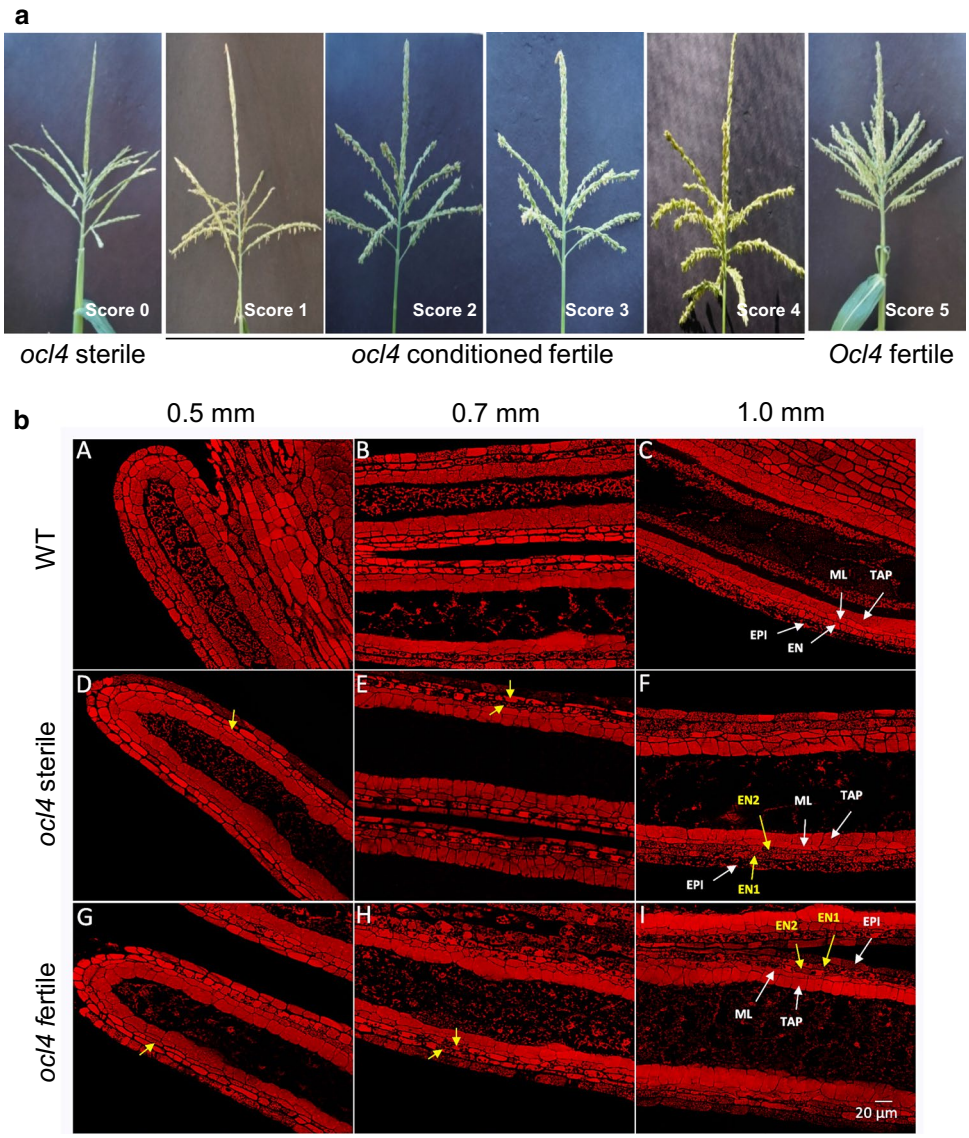

Fig. 2 Tassel phenotype and anther cell wall organization in *ocl4* mutants. **a** Representative maize tassels at the pollen shedding stage from normal fertile (*Ocl4*) and *ocl4//ocl4* mutants, depicting sterile (*ocl4* sterile from a segregating 1:1 family) and the range of conditioned fertile phenotypes. The scores represent fertility scores visually assigned on a scale of 0 to 5 (0 = sterile; 5 = wild type fertility). **b** Longitudinal confocal images of pre-meiotic anthers comparing fertile *Ocl4* and homozygous *ocl4//ocl4* mutants. Anthers of 0.5 mm, 0.7 mm, and 1.0 mm were dissected, fixed, stained with propidium iodide, and observed by confocal microscopy. Longitudinal confocal images of *Ocl4* fertile (labeled as WT) (**A–C**), *ocl4* sterile (**D–E**), and *ocl4* conditioned fertile (**G–I**) anthers at three developmental stages are presented. In *ocl4//ocl4* mutants, an extra cell layer with endothecial characteristics forms by periclinal division of the original endothecium (**D–E**, **G–H**); yellow arrowheads point to cells formed by extra periclinal division). Ultimately, *ocl4* lobes contain five somatic cell layers (**F** and **I**), in contrast to the four somatic cell layers found in normal *Ocl4* fertile lobes (**A–C**). Abbreviations: EPI, epidermis; EN, endothecium; ML, middle layer; TAP, tapetum; EN1 and EN2 represent two layers with endothecial characteristics. Scale bar: 20 µm

fertile samples (Fig. 3a). *Ocl4* is a key regulator of 21-nt phasiRNAs; when absent, phasiRNAs are almost negligible (Zhai et al. 2015). To find out whether phasiRNAs are also negligible in the conditioned fertile *ocl4* anthers, we selected the 359 most abundant phasiRNA precursors (from 359 *PHAS* loci) with a predicted miR2118 complementary site, from the previously published list (Zhai et al. 2015) to examine the proportion of 21-nt phasiRNAs among the 21-nt small RNA class across samples. The accumulation levels and the fraction of phasiRNAs were the highest in wild type as expected, but were also significantly higher in the conditioned fertile *ocl4* compared to *ocl4* sterile samples, suggesting a partial restoration of phasiRNAs in conditioned fertile plants (Fig. 3b).

Table 1 Derivation of lines used for phenotypic scoring, molecular analysis, and confocal microscopy

	PCR check	P1	PCR check	P2	PCR check	P3	PCR check	Uses
Conditioned fertile *ocl4* lines								
ZOO16	Yes	ZN57-17 ms × ZN57-38	Yes	ZM68-10 (×)	Yes	ZLL212 ms × ZLL212 *ocl4*	Yes	Phenotype, RNA extraction
ZOO19	Yes	ZN57-17 ms × 57–38 F	Yes	ZM68-10 (×)	Yes	ZLL212 ms × ZLL212 *ocl4*	Yes	Phenotype, RNA extraction
ZOO21	Yes	ZN58-17 (×)	Yes	ZM68-10 (×)	Yes	ZLL212 ms × ZLL212 *ocl4*	Yes	Phenotype, RNA extraction
ZQ8	No	ZM68-2 ms × ZM68-10	Yes					Phenotype, Confocal microscopy
Standard *ocl4* sterile lines								
ZO14	Yes	ZL11-3 ms × ZL fertile	No					Phenotype
ZQ4	No	ZP12 (×)	No	Three generations ms × F		ZLL212 ms × ZLL212 fertile *Ocl4*	Yes	Phenotype, Confocal microscopy

Conditioned fertile *ocl4* lines all trace back to individual ZLL212-1 (Online Resource 2 Table S1). PCR was used to validate genotype as described by Vernoud et al. (2009). ZOO lines were grown in the greenhouse; ZO and ZQ lines were field-grown. P refers to the prior parental generations. *ocl4* lines are homozygous for the mutant allele. Standard lines are maintained by crossing *ocl4//ocl4* male-sterile plants by *Ocl4//ocl4* heterozygotes (1:1 segregation fertile/sterile progeny) or by selfing heterozygotes (3:1 segregation)

We next explored phasiRNA accumulation from individual *PHAS* loci, as normally there is a wide variation in output. Out of 359 analyzed loci, most loci demonstrated negligible accumulation of phasiRNAs in *ocl4* mutants; however, there was a distinct subset of *PHAS* loci with significant accumulation of 21-nt phasiRNAs in conditioned fertile but not in *ocl4* sterile mutants (Fig. 3c). Although phasiRNAs are generated by sequential dicing of a *PHAS* locus transcript, there is unexpectedly a non-stoichiometric yield of 21-nt products: typically one dominant (most abundant) phasiRNA is produced per locus (Tamim et al. 2018). Focusing on the dominant products, we found an example in which the conditioned fertile samples accumulated higher product than the wild-type samples. From the analysis at the phasiRNA level, we observed the dominant phasiRNA (at position 13) to be highly abundant and three times higher in conditioned fertile samples (Fig. 3d). Therefore, while *Ocl4* is the key regulator of 21-nt phasiRNAs, warmer environmental conditions result in an increased accumulation of 21-nt phasiRNAs encoded by some loci.

Ago18b is significantly up-regulated in conditioned fertile *ocl4* anthers

One possible explanation for the low yield of 21-nt phasiRNAs in *ocl4* mutants is low accumulation of miR2118, the microRNA required for the initial cleavage of the primary transcripts. In a previous study of the *ms23* male-sterile maize mutant, there were few 24-nt phasiRNAs and miR2275 is nearly absent (Nan et al. 2017). Previously, low levels of miR2118 were found in sterile *ocl4* anthers (Zhai et al. 2015). These results implicate OCL4 as a major direct or indirect regulator of miR2118 biogenesis. In re-evaluating miR2118 in *ocl4*, we paradoxically found about a fourfold reduction in *ocl4* sterile anthers, but a 20-fold reduction in conditioned fertile *ocl4* anthers (Fig. 4a). Interestingly, in *Ocl4*, multiple miR2118 family isoforms accumulated, while in the conditioned fertile *ocl4* anthers, two-thirds of the overall abundance of the miR2118 family corresponded to just miR2118b (Fig. 4a). Because miR2118b is the major contributor of miR2118 overall abundance, we suspect it to be the isoform responsible for triggering the 21-nt phasiRNAs. We next re-evaluated the impact of *ocl4* on the accumulation of transcripts from the 359 21-nt *PHAS* loci whose phasiRNA products were analyzed in the previous section. We confirmed that the *ocl4* mutation caused significant reduction in the overall abundance of *PHAS* precursor transcripts (Zhai et al. 2015). This reduction was less pronounced in conditioned fertile *ocl4* as compared to sterile *ocl4*. Further, at the level of individual loci, there were clear differences in accumulation between the sterile and fertile versions of the *ocl4* mutants (Fig. 4b; Online Resource 1 Fig. S3).

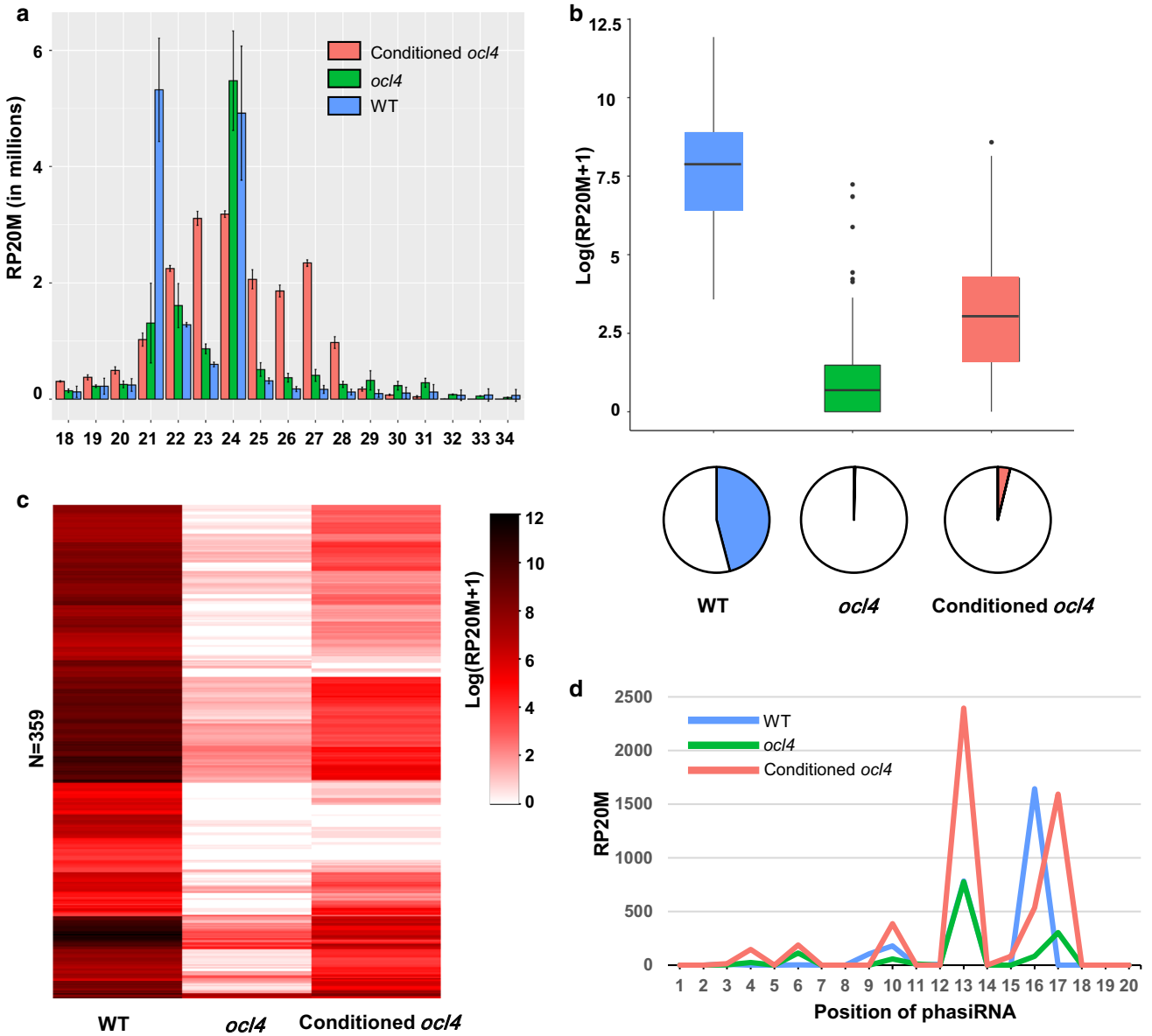

Fig. 3 Conditioned fertile *ocl4* plants show relatively higher accumulation of phasiRNAs compared to *ocl4* sterile plants. **a** Bar plot showing abundance distribution of different size classes (18 to 34 nt in length) of small RNAs in wild type, *ocl4*, and conditioned fertile *ocl4* anthers. **b** Boxplot (top) displaying 21-nt phasiRNA abundance distribution and pie chart (bottom) showing the fraction of 21-nt phasiRNA abundance out of the total abundance of all the small RNA population. **c** Heatmap displaying the accumulation of phasiRNAs from 359 analyzed phasiRNA precursors. **d** Line plot showing the accumulation of phasiRNAs on precursor for 20 positions starting from the cleavage site. RP20M stands for reads per 20 million reads. Samples used: for wild type ($N=3$) anthers of length 0.4 mm were used, for *ocl4* ($N=2$) and *ocl4* conditioned fertile ($N=2$) a mixture of anthers ranging from 0.4 and 0.7 mm in length were used

To extend our investigation of changes in factors that may be involved in 21-nt phasiRNA activities, we directed our focus to two additional aspects of the phasiRNA pathway. First, as noted previously, nine family members of HD-ZIP IV transcription factors, *Ocl4* included, are expressed in immature tassels. We hypothesized that in *ocl4* samples, one or a combination of the remaining eight factors could act as a substitute. Second, if there are any "functional" phasiRNAs produced in the conditioned fertile *ocl4* samples, we would expect to see expression of Argonaute proteins (Vazquez et al. 2004) involved in the loading of phasiRNAs. To address these hypotheses, we performed a pairwise differential expression analysis between wild-type, *ocl4* sterile, and *ocl4* conditioned fertile samples. Specifically, we focused on *Ocl4* and its eight relatives, nine *Ago* members (*Ago1a*, *b, c, d/ Ago5a*, *b*, *c/ Ago18a*, *b*) and two *Dcl* loci (*Dcl4* and *Dcl5*). Overall, we found *Ago18b* to be the most

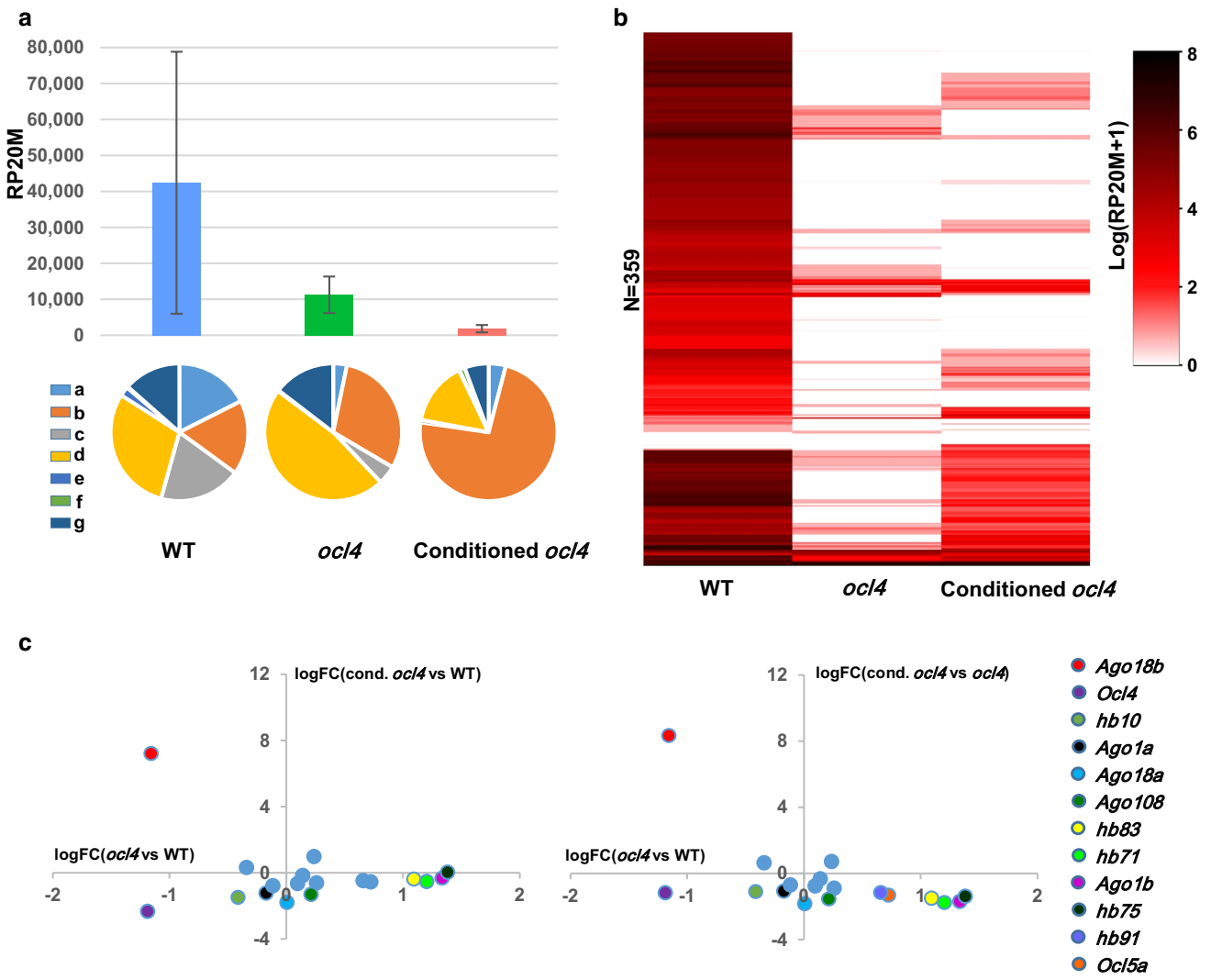

Fig. 4 *Ocl4* controls key players that are upstream or downstream of the produced phasiRNAs. **a** Bar plot (top) showing total abundance of miR2118 family and pie chart (bottom) showing the fraction contribution of each family member between wild type, *ocl4*, and conditioned fertile *ocl4* anthers. Characters a, b, c, d, e, f, g represent miR2118 members: miR2118a, miR2118b, etc. **b** Heatmap displaying the expression of 359 phasiRNA precursors. **c** Dot plot highlighting differential expression of key phasiRNA biogenesis pathway genes and some of the homeodomain leucine zipper type IV (HD-ZIP IV) tassel-specific genes. Genes that are significantly differentially expressed using a log-fold change cutoff of 1 are displayed with a unique color, while the rest are displayed by a blue color

significantly differentially expressed gene with about 8 log fold increase in the *ocl4* conditioned fertile compared to the sterile samples (Fig. 4c; Online Resource 2 Tables S3a, b, c). Moreover, we found seven of the nine HD-ZIP IV transcription factors (*Ocl4* included) to be differentially expressed; however, together with *Ocl4*, all were down-regulated in the *ocl4* samples, suggesting that none of these was acting as a substitute for *Ocl4*. Both *Dcl4* and *Dcl5* appear to be expressed relatively similarly across the samples and did not meet the cutoff as significantly differentially expressed genes.

Differential expression analysis uncovers distinct profile of genes for heat stress response and plastid differentiation

Is the overall transcriptome impacted differentially in conditioned fertile *ocl4* anthers compared to the *ocl4* sterile tissue? Evidence of a global impact on transcript accumulation in the conditioned fertile case would strengthen our view that these anthers are substantially different. We analyzed the RNA-seq reads from *Ocl4* and from the two classes of *ocl4* 0.4–0.7 mm anthers: most genes were expressed in all three conditions (Fig. 5a). While there is a substantial

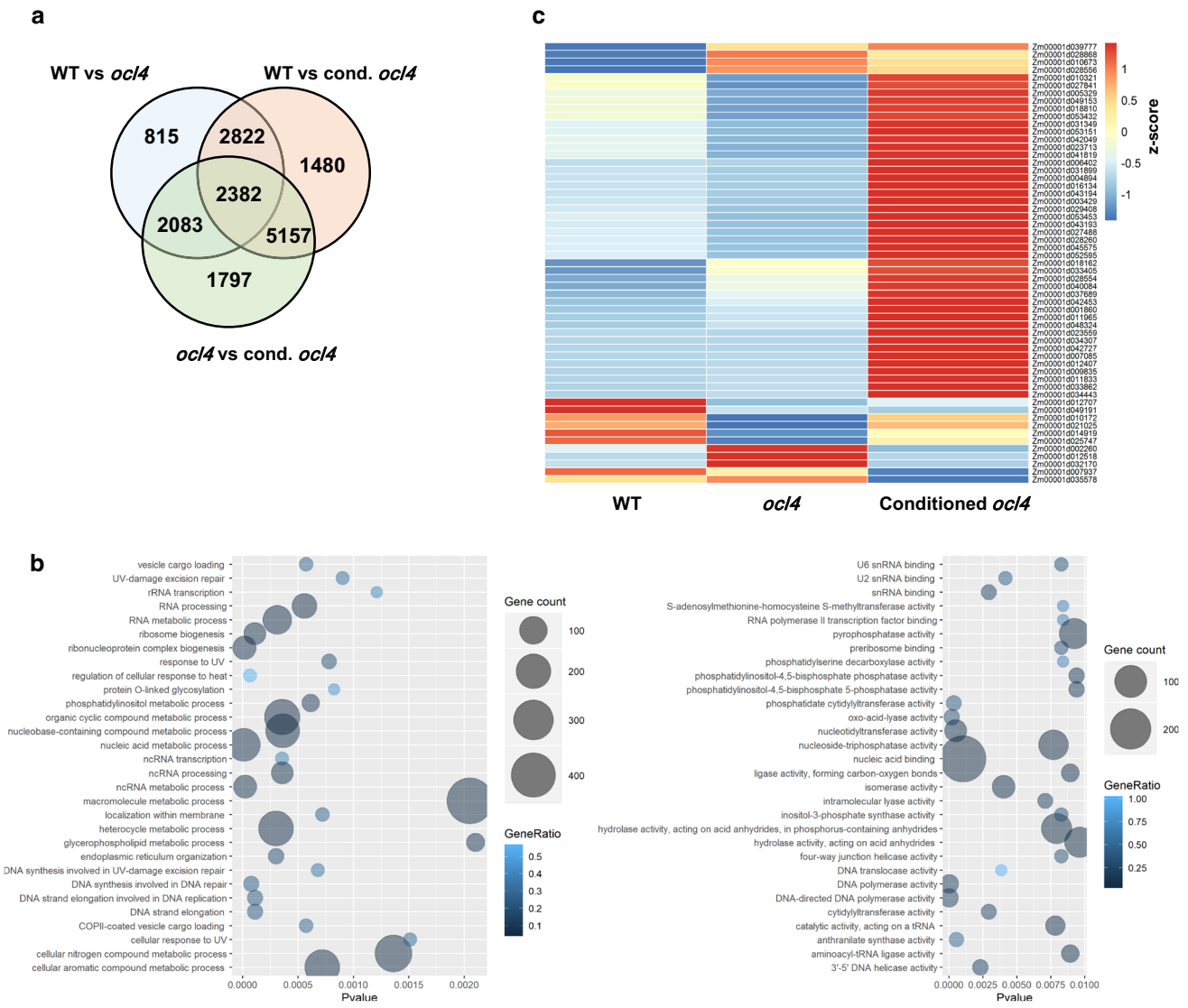

Fig. 5 Conditioned fertile *ocl4* anthers have distinct profile of genes for plastid differentiation and heat stress response. **a** Venn diagram showing the overlap of genes that are differentially expressed between three pairwise differential expression analysis between wild type, *ocl4*, and conditioned fertile *ocl4* samples. **b** Top 30 biological processes (left) and molecular functions (right) that are enriched from Gene ontology (GO) analysis of genes that are uniquely differentially expressed between *ocl4* and conditioned *ocl4* samples. **c** Heatmap highlighting 57 differentially expressed genes from the set of 238 previously published nuclear genes involved in plastid differentiation

overlap (~ 5000) between genes that are differentially expressed between *ocl4* sterile and *ocl4* conditioned fertile samples relative to the wild type, there are ~ 1800 genes that are uniquely differentially expressed in either *ocl4* or conditioned fertile *ocl4* samples. To find out more about the overall differentially expressed genes in conditioned fertility, we performed a Gene Ontology (GO) analysis to search for processes that these genes play a role in. Interestingly, we found genes to be significantly enriched in processes that are linked to regulation of cellular response to heat. Other processes such as cellular response to environmental stimulus, cellular response to abiotic stimulus, and cellular response to ultra violet radiation also show up in the GO analysis (Fig. 5b; Online Resource 1 Fig. S4, Online Resource 2 Tables S4a, b, c). Furthermore, the presence of chloroplasts is a key characteristic of normal endothecial cells by the 1.0 mm anther stage accompanied by expression of nuclear genes involved in plastid differentiation (Murphy et al. 2015). We analyzed expression of a set of 238 nuclear genes that produce proteins localized to plastids in *Ocl4* normal, sterile, and conditioned fertile pre-meiotic maize anthers; 57 genes were found to be significantly differentially expressed (Fig. 5c). The GO analysis of plastid-related genes revealed significant enrichment of genes involved in metabolic processes and catalytic activity (Online Resource 2 Tables S5a, b, c).

Discussion

We used fertility classification, microscopy, genetics, and transcriptional analysis to characterize the maize *ocl4* mutant in which conditioned male fertility can occur. Conditioned fertility may be ascribed, at least in part, to a positive response to elevated temperature (Online Resource 2 Table S1). Collectively, the data presented here and prior observations (Zhai et al. 2015) demonstrate that the 21-nt class of phasiRNAs peaks in abundance in 0.4 mm anthers, during the loss of pluripotency in the newly specified somatic cells. These small RNAs are highly abundant through the 1.0 mm stage, when their precursor transcripts and the trigger miR2118 have decreased substantially. This suggests that there is a narrow developmental window during which 21-nt phasiRNAs are generated and that they have a relatively long lifespan. We observed that the biogenesis of 21-nt phasiRNAs is largely dependent on *Ocl4* at three key steps: (1) production of *PHAS* precursor transcripts (Fig. 4b), (2) expression of individual miR2118 loci (Fig. 4a), and (3) accumulation of 21-nt phasiRNAs (Fig. 3c). All three sets of RNAs were greatly reduced in sterile pre-meiotic anthers of the *ocl4* mutant, confirming a previous report (Zhai et al. 2015). The total 21-nt small RNAs dropped by ~46% and ~38% in sterile and fertile *ocl4* anthers, respectively (Fig. 3a). The major classes of the reduced-abundance small RNAs include miR2118 family members (Fig. 4a) and 21-nt phasiRNAs (Fig. 3b). Besides the small RNA classes specifically linked to the biogenesis of 21-nt phasiRNAs, miR159, miR408, miR168, and miR2275 accumulation levels were much higher in conditioned fertile *ocl4* (Online Resource 1 Fig. S5). These changes indicate that OCL4 plays a major role in 21-nt phasiRNA biogenesis during the pre-meiotic stage of maize anther development.

Surprisingly, in sterile *ocl4* anthers, we observed a subset of *PHAS* loci that are expressed at approximately normal levels, plus there is a low level of miR2118 accumulation, and 21-nt phasiRNAs are still present. It therefore seems possible that a small proportion of 21-nt phasiRNA production is controlled by a different transcription factor than OCL4. This possibility is reinforced by analysis of the conditioned fertile *ocl4* anthers: there was a partial restoration of 21-nt phasiRNAs (Fig. 3c), heightened expression of miR2118b (Fig. 4c), and normal accumulation of some *PHAS* precursor types and ectopic expression of a unique locus (at position 13) (Fig. 3d).

Another explanation for lower 21-nt phasiRNA levels in *ocl4* is that the *21-PHAS* precursors are less efficiently processed into 21-nt phasiRNAs, because there is reduced abundance of miR2118 in fertile *ocl4* (Fig. 4a). The level of *Dcl4* transcripts was essentially the same in all genotypes (Fig. 4c), while the *21-PHAS* precursor transcripts were moderately increased in fertile *ocl4* (Fig. 4b). Furthermore, there was no significant change in the phasing pattern among the genotypes and phenotypes that we analyzed (Fig. 3d), indicating that no miRNA trigger other than miR2118 initiates 21-nt phasiRNA production. Our studies raise interesting questions for future analysis. Why is there higher expression of *Ago18b* and less miR2118 in the fertile *ocl4*? Further chromatin immunoprecipitation (ChIP) studies will be required to answer such questions and to determine, for example, whether increased AGO1b protein in sterile *ocl4* stabilized miR2118 and therefore "increased" the abundance.

Our data also confirmed the observation that 24-nt phasiRNA abundances in *ocl4* are largely unchanged relative to the sibling *Ocl4* fully fertile plants (Zhai et al. 2015). We found only moderate fluctuations in *ocl4*, 17% higher in sterile and 32% lower in fertile pre-meiotic anthers, and these levels correlated with *Dcl5* transcript levels (Fig. 4c). We conclude that OCL4 is unlikely to directly function in the 24-nt phasiRNA pathway.

These results suggest that OCL4 is responsible for the regulation of biogenesis of most, but not all 21-nt phasiRNAs. We have evidence of normal or higher accumulation of specific 21-nt phasiRNAs, a miR2118 isoform, and 21-nt *PHAS* transcript in *ocl4* mutants. In the conditioned fertile *ocl4* plants, these features are elevated relative to the *ocl4* sterile individuals. Based on these observations, it is likely that the OCL4 transcription factor is responsible for regulating most loci involved in 21-nt phasiRNA biogenesis, but there is a subclass regulated independently. Furthermore, this subclass is up-regulated in conditioned male-fertile *ocl4* anthers. We tested the logical possibility that another HD-ZIP IV transcription factor could explain these phenomena but found there are no HD-ZIP IV transcription factors that are up-regulated in *ocl4* conditioned fertile samples. Interestingly, we found that *Ago18b* is significantly up-regulated in the conditioned fertile samples (Fig. 4c). It is known that AGO18b is highly expressed in maize tassels during meiosis and it negatively controls determinacy of spikelet meristems. AGO18b primarily binds to 21-nt phasiRNAs in the pre-meiotic tassels (Sun et al. 2019). Knockdown of *Ago18* results in male sterility and reduction in phasiRNAs in rice (Das et al. 2020). Thus, it is possible that restoration of 21-nt phasiRNAs in conditioned fertile *ocl4* anthers might result from AGO18b accumulation, which may be independently stabilizing a subclass of 21-nt phasiRNAs.

The possibility of an epigenetic component to conditioned male fertility mediated by *ocl4* remains an open question for future analysis. It is also possible that parental environment can establish epigenetic states that influence multiple generations (Heard and Martienssen 2014). Environmentally induced *trans*-generational epigenetic inheritance is an emerging field (Casier et al. 2019; Pang et al.

2019). The scientific understanding of myriad mechanisms, especially the role of reproductive small RNAs in *trans*-generational inheritance of male fertility and sterility, is at a nascent stage. In the nematode, *C. elegans,* piRNAs are capable of triggering a multigenerational epigenetic memory in the germline (Ashe et al. 2012). Yet, studies implicating reproductive small RNAs in environmentally regulated or "conditioned" fertility are absent in mammals and rare in plants. Future studies focused on epigenetic factors and histone and DNA epigenetic marks using *ocl4* plants grown under controlled conditions could test the hypothesis that parental growth environment establishes the propensity for full sterility or partial fertility of *ocl4* mutants.

Materials and methods

Plant materials and growing conditions

V. Vernoud donated an *ocl4* stock introgressed in inbred A188 (Vernoud et al. 2009), and I. Golubovskaya (UC Berkeley) derived a stock segregating 1:1 for *ocl4* (*ocl4//ocl4* male-sterile × *ocl4//+* maintainer) that was donated to Stanford University. This stock was maintained over three generations with 1:1 segregation and used in 55 complementation tests with newly identified male-sterile mutants (Timofejeva et al. 2013). Because we observed excess male sterility in five complementation tests involving a new, uncloned, and apparently unrelated mutant, *tapetal cell layers 1* (*tcl1*), the F_2 progenies of its complementation tests were re-evaluated in the greenhouse, including one family from the cross *ocl4//ocl4* × *tcl1/+,* followed by self-pollination. One set of progeny were grown in the greenhouse and genotyped by polymerase chain reaction (PCR) (Vernoud et al. 2009); two homozygous *ocl4* progeny were male sterile as expected, but two were fully fertile. The fertile individuals were successfully self-pollinated and crossed onto *ocl4* male-sterile ears; all progeny should have been *ocl4* homozygotes. In the 2014 field season, seeds of one selfed individual were planted as ZM68, and 80% of the progeny were fertile (24F:6 ms); each plant in this family was test-crossed to *tcl1//tcl1* male-sterile plants to identify individuals that were not carrying *tcl1* (Online Resource 2 Table S1). Individual ZM68-10 was not a carrier of *tcl1* and its self-pollination progeny and progeny from a cross onto sibling male-sterile ZM68-2 were selected for further analysis in subsequent field seasons. All plants were genotyped to confirm that they were *ocl4//ocl4* double mutant homozygotes, and this was checked for at least two generations. As described above, in 2013, the test cross with the *tcl1* mutant, in which the *ocl4//ocl4* male-sterile female was crossed by a heterozygous *tcl1//+* male, was field-grown as family ZL57; all progeny were fertile, as expected, and self-pollination was performed to generate families expected to segregate 1:2:1 for *ocl4*. The first instance of fertility in an *ocl4* homozygote was in the greenhouse generation of 2013 (ZLL212 family). At the "ZLL" generation, greenhouse-grown plants were genotyped using a published PCR-based protocol (Vernoud et al. 2009), and two homozygous *ocl4//ocl4* fertile plants were identified (Online Resource 2 Table S1). Progeny of these individuals were grown in subsequent field seasons, genotyped again at most generations to verify homozygosity for *ocl4*. Some field seasons experienced late June heat waves corresponding to the time period of early anther development with abundant 21-nt phasiRNAs. Heat wave conditions correspond to three or more days in a row of 32 °C or higher; night temperatures on such days are also higher than normal by several degrees. Historic weather data were retrieved from the Weather Underground dataset (https://www.wunderground.com/history) using the station closest (2 km) from the Stanford field site (37°25′45.9"N, 122°10′52.5"W).

Anther collections and confocal microscopy

Anthers were dissected and staged by length using a micrometer and dissecting microscope. For RNA extraction, a total of 50 anthers of the target length (0.4 to 0.7 mm) were pooled from one immature tassel of each of the conditioned fertile *ocl4* plants grown under controlled conditions in greenhouse at Stanford, CA. All anthers were transferred to chilled vials immersed in liquid nitrogen and then stored at -80 °C until further use. For confocal microscopy, anthers of 0.5 mm, 0.7 mm, and 1.0 mm were dissected and stored in 100% ethanol at 4 °C. Propidium iodide staining and confocal imaging utilized published protocols (Kelliher and Walbot 2011).

sRNA-seq and RNA-seq library construction and sequencing

Total RNA for sRNA-seq and RNA-seq libraries was isolated using the TRI Reagent RNA isolation reagent (Sigma-Aldrich) following the manufacturer's instructions. Total RNA quality was assessed using the Agilent RNA 6000 Pico Kit (Agilent). For library preparation, 20 to 30 nt RNAs were excised from a 15% polyacrylamide/urea gel, and ~ 25 ng of sRNA was used for library construction with the TruSeq Small RNA Prep Kit (Illumina) following the manufacturer's instructions. For RNA-seq, 2 µg of total RNA was treated with DNase I (New England BioLabs) and then cleaned with RNA Clean and Concentrator-5 (Zymo Research). The TruSeq Stranded Total RNA with RiboZero-Plant Kit (Illumina) or NEBNext Ultra II Directional RNA Library Prep Kit (New England BioLabs) was used for library construction with 500 ng of treated RNA, following the manufacturer's instructions. Sequencing in single-end mode on an Illumina HiSeq 2500 (University of Delaware) yielded 51 nt reads for both sRNA-seq and RNA-seq.

Data handling and bioinformatics

sRNA-seq data were processed as previously described (Mathioni et al. 2017). Briefly, we first used Trimmomatic (v0.32) (Bolger et al. 2014) to remove the linker adaptor sequences. Trimmed reads are then chopped to reads that are within 18 to 34 nt length before they were mapped to version 4 of the B73 maize genome using Bowtie (Langmead et al. 2009). Read counts were normalized to 20 million to allow for the direct comparison across libraries and were hit normalized to account for reads that map to multiple genomic positions. For phasiRNA analysis, we used the list of 463 previously reported *PHAS* loci (Zhai et al. 2015) and selected 359 *PHAS* loci with a miR2118 target site. For RNA-seq libraries, reads were first trimmed for adapter using Trimmomatic and then mapped to version 4 of the B73 genome using Tophat v2 (Trapnell et al. 2009). Read counts were then generated using featureCounts (Liao et al. 2014), and the differential expression analyses were performed using DESeq2 (Love et al. 2014) package in R.GO analyses was done using PANTHER (Mi et al. 2019).

Author contribution statements VW conceived of the project and derived line(s) reported here, which were genotyped by HZ. PY collected staged anthers for RNA analysis and evaluated fertility status; XZ acquired confocal images; CT made libraries and ST analyzed sequencing reads. PY and ST interpreted the data in consultation with VW and wrote the manuscript, which was improved and edited by VW and BCM. All authors provided critical feedback and helped shape the research, analysis, and final manuscript.

Supplementary Information The online version contains supplementary material available at https://doi.org/10.1007/s00497-021-00406-3.

Funding This study was supported by U.S. National Science Foundation Plant Genome Research Project (Award # 1754097) to BCM and VW. PY was supported by a Fulbright-Nehru grant from United-States India Educational Foundation (Award No. 2200/FNPDR/2016).

Availability of data and materials The data reported in this paper have been deposited in the Gene Expression Omnibus (GEO) database, Series GSE150446, accession nos. GSM4550675 to GSM4550682 for RNA-seq data, GSM4550683 to GSM4550690 for small RNA data.

Code availability Not applicable.

Compliance with ethical standards

Conflicts of interest The authors declare that they have no conflict of interest.

Consent to participate Not applicable.

Consent for publication All the authors read and approved the manuscript for publication.

Ethics approval Not applicable.

References

Ashe A, Sapetschnig A, Weick EM, Mitchell J, Bagijn MP, Cording AC, Doebley AL, Goldstein LD, Lehrbach NJ, Le Pen J, Pintacuda G (2012) piRNAs can trigger a multigenerational epigenetic memory in the germline of *C. elegans*. Cell 150:88–99

Bai JF, Wang YK, Wang P, Duan WJ, Yuan SH, Sun H, Yuan GL, Ma JX, Wang N, Zhang FT, Zhang LP (2017) Uncovering male fertility transition responsive miRNA in a wheat photothermosensitive genic male sterile line by deep sequencing and degradome analysis. Front Plant Sci 8:1370

Bolger AM, Lohse M, Usadel B (2014) Trimmomatic: a flexible trimmer for Illumina sequence data. Bioinformatics 30:2114–2120

Casier K, Boivin A, Carré C, Teysset L (2019) Environmentally-induced transgenerational epigenetic inheritance: implication of PIWI interacting RNAs. Cells 8:1108. https://doi.org/10.3390/cells8091108

Chen R, Zhao X, Shao Z, Wei Z, Wang Y, Zhu L, Zhao J, Sun M, He R, He G (2007) Rice UDP-glucose pyrophosphorylase1 is essential for pollen callose deposition and its cosuppression results in a new type of thermosensitive genic male sterility. Plant Cell 19:847–861

Chen X, Hu J, Zhang H, Ding Y (2014) DNA methylation changes in photoperiod-thermo-sensitive male sterile rice PA64S under two different conditions. Gene 537:143–148

Das S, Swetha C, Pachamuthu K, Nair A, Shivaprasad PV (2020) Loss of function of *Oryza sativa* Argonaute 18 induces male sterility and reduction in phased small RNAs. Plant Reprod 33:59–73

Ding J, Lu Q, Ouyang Y, Mao H, Zhang P, Yao J, Xu C, Li X, Xiao J, Zhang Q (2012a) A long noncoding RNA regulates photoperiod-sensitive male sterility, an essential component of hybrid rice. Proc Natl Acad Sci 109:2654–2659

Ding J, Shen J, Mao H, Xie W, Li X, Zhang Q (2012b) RNA-directed DNA methylation is involved in regulating photoperiod-sensitive male sterility in rice. Mol Plant 5:1210–1216

Dukowic-Schulze S, van der Linde K (2021) Oxygen, secreted proteins and small RNAs: mobile elements that govern anther development. Plant Reprod. https://doi.org/10.1007/s00497-020-00401-0

Fan Y, Yang J, Mathioni SM, Yu J, Shen J, Yang X, Wang L, Zhang Q, Cai Z, Xu C, Li X, Xiao J, Meyers BC, Zhang Q (2016) PMS1T, producing phased small-interfering RNAs, regulates photoperiod-sensitive male sterility in rice. Proc Natl Acad Sci 113:15144–15149

Heard E, Martienssen RA (2014) Transgenerational epigenetic inheritance: myths and mechanisms. Cell 157:95–109

Javelle M, Klein-Cosson C, Vernoud V, Boltz V, Maher C, Timmermans M, Depège-Fargeix N, Rogowsky PM (2011) Genome-wide characterization of the HD-ZIP IV transcription factor family in maize: preferential expression in the epidermis. Plant Physiol 157:790–803

Jiang P, Lian B, Liu C, Fu Z, Shen Y, Cheng Z, Qi Y (2020) 21-nt phasiRNAs direct target mRNA cleavage in rice male germ cells. Nat Commun 11:5191. https://doi.org/10.1038/s41467-020-19034-y

Johnson C, Kasprzewska A, Tennessen K, Fernandes J, Nan G, Walbot V, Sundaresan V, Vance V, Bowman LH (2009) Clusters and

superclusters of phased small RNAs in the developing inflorescence of rice. Genome Res 19:1429–1440
Kelliher T, Walbot V (2011) Emergence and patterning of the five cell types of the *Zea mays* anther locule. Dev Biol 350:32–49
Kelliher T, Walbot V (2014) Germinal cell initials accommodate hypoxia and precociously express meiotic genes. Plant J 77:639–652
Kim YJ, Zhang D (2018) Molecular control of male fertility for crop hybrid breeding. Trends Plant Sci 23:53–65
Langmead B, Trapnell C, Pop M, Salzberg SL (2009) Ultrafast and memory-efficient alignment of short DNA sequences to the human genome. Genome Biol 10:R25
Liao Y, Smyth GK, Shi W (2014) featureCounts: an efficient general purpose program for assigning sequence reads to genomic features. Bioinformatics 30:923–930
Li H, Yuan Z, Vizcay-Barrena G, Yang C, Liang W, Zong J, Wilson ZA, Zhang D (2011) PERSISTENT TAPETAL CELL1 encodes a PHD-finger protein that is required for tapetal cell death and pollen development in rice. Plant Physiol 156:615–630
Love MI, Huber W, Anders S (2014) Moderated estimation of fold change and dispersion for RNA-seq data with DESeq2. Genome Biol 15:550
Mathioni SM, Kakrana A, Meyers BC (2017) Characterization of plant small RNAs by next generation sequencing. Curr Protoc Plant Biol 2:39–63
Mi H, Muruganujan A, Ebert D, Huang X, Thomas PD (2019) PANTHER version 14: more genomes, a new PANTHER GO-slim and improvements in enrichment analysis tools. Nucleic Acids Res 47:D419–D426
Murphy KM, Egger RL, Walbot V (2015) Chloroplasts in anther endothecium of *Zea mays* (Poaceae). Am J Bot 102:1931–1937
Nan G-L, Zhai J, Arikit S, Morrow D, Fernandes J, Mai L, Nguyen N, Meyers BC, Walbot V (2017) MS23, a master basic helix-loop helix factor, regulates the specification and development of tapetum in maize. Development 144:163–172
Pang YY, Lu RJ, Chen PY (2019) Behavioral epigenetics: perspectives based on experience-dependent epigenetic inheritance. Epigenomes 3:18. https://doi.org/https://doi.org/10.3390/epigenomes3030018
Qi Y, Liu Q, Zhang L, Mao B, Yan D, Jin Q, He Z (2014) Fine mapping and candidate gene analysis of the novel thermo-sensitive genic male sterility tms9-1 gene in rice. Theor Appl Genet 127:1173–1182
Sosso D, Wisniewski JP, Khaled AS, Hueros G, Gerentes D, Wyatt P, Rogowksy PM (2010) The *Vpp1*, *Esr6a*, *Esr6b*, and *OCL4* promoters are active in distinct domains of maize endosperm. Plant Sci 179:86–96. https://doi.org/https://doi.org/10.1016/j.plantsci.2010.04.006
Sun W, Chen D, Xue Y, Zhai L, Zhang D, Cao Z, Liu L, Cheng C, Zhang Y, Zhang Z (2019) Genome-wide identification of AGO18b-bound miRNAs and phasiRNAs in maize by cRIP-seq. BMC Genomics 20:656
Tamim S, Cai Z, Mathioni SM, Zhai J, Teng C, Zhang Q, Meyers BC (2018) Cis-directed cleavage and nonstoichiometric abundances of 21-nucleotide reproductive phased small interfering RNAs in grasses. New Phytol 220:865–877
Teng C, Zhang H, Hammond R, Huang K, Meyers BC, Walbot V (2020) *Dicer-like 5* deficiency confers temperature-sensitive male sterility in maize. Nat Commun 11:2912
Timofejeva L, Skibbe DS, Lee S, Golubovskaya I, Wang R, Harper L, Walbot V, Cande WZ (2013) Cytological characterization and allelism testing of pre-meiotic anther developmental mutants identified in a screen of maize male sterile lines. G3:231–249
Trapnell C, Pachter L, Salzberg SL (2009) TopHat: discovering splice junctions with RNA-Seq. Bioinformatics 25:1105–1111
Vazquez F, Vaucheret H, Rajagopalan R, Lepers C, Gasciolli V, Mallory AC, Hilbert JL, Bartel DP, Crete P (2004) Endogenous trans-acting siRNAs regulate the accumulation of Arabidopsis mRNAs. Mol Cell 16:69–79
Vernoud V, Laigle G, Rozier F, Meeley RB, Perez P, Rogowsky PM (2009) The HD-ZIP IV transcription factor OCL4 is necessary for trichome patterning and anther development in maize. Plant J 59:883–894
Wang C-JR, Nan GL, Kelliher T, Timofejeva L, Vernoud V, Golubovskaya IN, Harper L, Egger RL, Walbot V, Cande WZ (2012) Maize *multiple archesporial cell 1 (mac1)*, an ortholog of rice *TDL1A*, modulates cell proliferation and identity in early anther development. Development 39:2594–2603
Xia R, Chen C, Pokhrel S, Ma W, Huang K, Patel P, Wang F, Xu J, Liu Z, Li J, Meyers BC (2019) 24-nt reproductive phasiRNAs are broadly present in angiosperms. Nat Commun 10:627
Zhai J, Zhang H, Arikit S, Huang K, Nan GL, Walbot V, Meyers BC (2015) Spatiotemporally dynamic, cell-type–dependent premeiotic and meiotic phasiRNAs in maize anthers. Proc Natl Acad Sci 112:3146–3151
Zhang H, Liang W, Yang X, Luo X, Jiang N, Ma H, Zhang D (2010) Carbon starved anther encodes a MYB domain protein that regulates sugar partitioning required for rice pollen development. Plant Cell 22:672–689
Zhang H, Xu C, He Y, Zong J, Yang X, Si H, Sun Z, Hu J, Liang W, Zhang D (2013) Mutation in CSA creates a new photoperiod-sensitive genic male sterile line applicable for hybrid rice seed production. Proc Natl Acad Sci 110:76–81
Zhang YC, Lei MQ, Zhou YF, Yang YW, Lian JP, Yu Y, Feng YZ, Zhou KR, He RR, He H, Zhang Z (2020) Reproductive phasiRNAs regulate reprogramming of gene expression and meiotic progression in rice. Nat Commun 11:6031. https://doi.org/10.1038/s41467-020-19922-3
Zheng Y, Wang Y, Wu J, Ding B, Fei Z (2015) A dynamic evolutionary and functional landscape of plant phased small interfering RNAs. BMC Biol 13:32
Zhou H, Liu Q, Li J, Jiang D, Zhou L, Wu P, Lu S, Li F, Zhu L, Liu Z, Chen L, Liu YG, Zhuang C (2012) Photoperiod- and thermo-sensitive genic male sterility in rice are caused by a point mutation in a novel noncoding RNA that produces a small RNA. Cell Res 2:649–660. https://doi.org/10.1038/cr.2012.28